

# Cooperative Cargo Transport by Several Molecular Motors

Stefan Klumpp and Reinhard Lipowsky  
*Max Planck Institute of Colloids and Interfaces,  
Science Park Golm, 14424 Potsdam, Germany*

## Abstract

The transport of cargo particles which are pulled by several molecular motors in a cooperative manner is studied theoretically. The transport properties depend primarily on the maximal number,  $N$ , of motor molecules that may pull simultaneously on the cargo particle. Since each motor must unbind from the filament after a finite number of steps but can also rebind to it again, the actual number of pulling motors is not constant but varies with time between zero and  $N$ . An increase in the maximal number  $N$  leads to a strong increase of the average walking distance (or run length) of the cargo particle. If the cargo is pulled by up to  $N$  kinesin motors, e.g., the walking distance is estimated to be  $5^{N-1}/N$  micrometers which implies that seven or eight kinesin molecules are sufficient to attain an average walking distance in the centimeter range. If the cargo particle is pulled against an external load force, this force is shared between the motors which provides a nontrivial motor-motor coupling and a generic mechanism for nonlinear force-velocity relationships. With increasing load force, the probability distribution of the instantaneous velocity is shifted towards smaller values, becomes broader, and develops several peaks. Our theory is consistent with available experimental data and makes quantitative predictions that are accessible to systematic in vitro experiments.

## I. INTRODUCTION

Cytoskeletal motors which perform active movements along cytoskeletal filaments drive the long-range transport of vesicles, organelles, and other types of cargo in biological cells. In the following, we will consider *processive* motors which can complete many chemo-mechanical cycles while remaining bound to the filaments. During the last decade, the properties of *single* processive motors such as kinesin on microtubules and myosin V on actin filaments have been characterized in some detail using *in vitro* motility assays and novel experimental techniques for the visualization and manipulation of single molecules [1, 2]. However, *in vivo*, force generation and transport is typically performed by *several* motor molecules in a cooperative fashion as revealed by electron microscopy [3, 4] and by tracking of the cargo particles with optical methods [5, 6, 7]. It has also been found that some cargo particles bind different types of motors simultaneously so that these particles can reverse their direction of motion along microtubules [5, 7] or switch from microtubules to actin filaments [8].

The force generated by a single cytoskeletal motor is rather small and of the order of a few piconewtons. Larger forces can be generated if several motors pull on the same cargo. This is necessary, e.g., for the fast transport of large organelles through the cytoplasm which is a highly viscous medium [9]. Likewise, large forces arising from many motors are also required for specific motor functions such as the extraction of membrane tubes from vesicles [10, 11].

Another important consequence of the cooperative action of several motors is that it increases the walking distance (or run length) of the cargo particles. Since the binding energy of such a cargo particle is necessarily finite, it can be overcome by thermal fluctuations which are ubiquitous in cells. If the cargo particle is pulled by a single processive motor, its walking distance is typically of the order of one micrometer [12]. If the cargo particle is pulled by several motors, the walking distance is strongly increased since the cargo continues to move along the filament unless all motors unbind simultaneously. In addition, as long as the cargo particle is still connected to the filament by at least one motor, all unbound motors can rebind rather fast, because they are prevented from diffusing away from the filament. It has also been shown using *in vitro* motility assays that cargo particles pulled by many motors can switch tracks and move along several filaments at the same time, so that huge walking distances

can be achieved which exceed the length of a single filament [13].

In this article, we study these cooperative transport phenomena from the theoretical point of view. First, we introduce a generic transition rate model for the transport of cargo particles, which are pulled by up to  $N$  motors, and obtain general expressions for the average number of pulling motors, for the average velocity of the bound cargo particle, for its effective unbinding rate, and for the distribution of its walking distances. Next, we focus on the case of cargo particles with a dilute motor coverage, which should be directly applicable to typical bead assays. In the absence of an external load force, we obtain an explicit expression for the average walking distance of the cargo particles. Using this expression for particles that are pulled by up to  $N$  kinesin motors, we estimate the walking distance to grow as  $5^{N-1}/N$ . We also calculate the distribution of the walking distances which is found to exhibit a tail with an extended plateau region for  $N \geq 3$ .

An external load force leads to a nontrivial coupling between the different motors because the unbinding rates of the motors increase with increasing force. As a consequence, the average number of bound motors decreases as the load force is increased which provides a generic mechanism for *nonlinear* force-velocity relationships. We argue that the motor transport becomes ineffective at a critical force for which the average walking distance becomes comparable with the step size of a single motor. For  $N \geq 2$ , this critical force is found to be small compared to the maximal stall force which can be sustained by  $N$  motors. Finally, we calculate the probability distribution of the instantaneous velocity of the bound cargo particle. As the load force is increased, this velocity distribution is shifted towards smaller values, becomes broader, and develops several peaks.

We will focus on the transport by kinesin motors, which pull cargo particles along microtubules, since, in this case, all input parameters for our theory have been determined experimentally, but our analysis is rather general and can be applied to other types of cytoskeletal motors as well. All experimental data that are available for cargo transport by several kinesin motors are consistent with our theoretical results.

## II. MODEL AND GENERAL SOLUTION

**Transition rate model.** We consider cargo particles which are pulled by  $N$  motors, see Fig. 1. These motors are irreversibly attached to the cargo particle, but can bind to and unbind from the filament along which they move. Thus, the number  $n$  of motor molecules that are bound to the filament can vary between  $n = 0$  and  $n = N$ . We will distinguish  $N + 1$  different states of the cargo particle corresponding to the unbound state with  $n = 0$  and to  $N$  bound states with  $n = 1, 2, \dots, N$ . Each of these bound states contains  $N!/(N - n)!n!$  substates corresponding to the different combinations of connecting  $n$  motor molecules to the filament. If the cargo particle is linked to the filament through  $n$  motors, it moves with velocity  $v_n$ . Unbinding of a motor from the filament and binding of an additional motor to the filament occur with rates  $\epsilon_n$  and  $\pi_n$ , respectively.

We first derive general expressions for the transport properties of the cargo particles pulled by  $N$  motors without specifying how the rates  $\epsilon_n$  and  $\pi_n$  and the velocities  $v_n$  depend on the number  $n$  of bound motors. We derive the distributions of the number of bound motors, of the binding times and of the walking distances from which we then obtain the effective unbinding rate, the average walking distance, and the average velocity. All these quantities can be directly measured by particle tracking both in vivo and in vitro.

**Distribution of the number of bound motors.** We first calculate the distribution of the number of bound motors. We denote by  $P_n$  the probability that the cargo particle is in state  $|n\rangle$ , i.e. bound to the filament by  $n$  motors. These probabilities satisfy the master equation

$$\frac{\partial}{\partial t} P_n = \epsilon_{n+1} P_{n+1} + \pi_{n-1} P_{n-1} - (\epsilon_n + \pi_n) P_n. \quad (1)$$

We are interested in the transport properties of bound cargo particles. Since all movements of bound cargo particles begin and end with  $n = 0$ , every step from state  $|n\rangle$  to  $|n + 1\rangle$  implies a backward step at some later time. To determine the transport properties of the bound cargo particles, we can therefore focus on the stationary solution of the master equation which is characterized by

$$\epsilon_{n+1} P_{n+1} = \pi_n P_n \quad (2)$$

for  $0 \leq n \leq N - 1$ .

Expressing subsequently all  $P_n$  in terms of  $P_0$  and using the normalization  $\sum_{n=0}^N P_n = 1$ , we obtain

$$P_0 = \left[ 1 + \sum_{n=0}^{N-1} \prod_{i=0}^n \frac{\pi_i}{\epsilon_{i+1}} \right]^{-1} \quad \text{and} \quad P_n = P_0 \prod_{i=0}^{n-1} \frac{\pi_i}{\epsilon_{i+1}}. \quad (3)$$

To determine the transport properties of cargo particles bound to the filament, we normalize these probabilities with respect to the bound states, i.e. we consider the the probabilities  $P_n/(1 - P_0)$  that a bound cargo particle is bound to the filament by  $n$  motors. For example, the average number of bound motors is given by

$$N_b = \sum_{n=1}^N n P_n / (1 - P_0). \quad (4)$$

**Average velocity.** The distribution of the number of bound motors as given by Eq. (3) implies the distribution of velocities of the cargo particle moving along the filament

$$P(v) = \sum_{n=1}^N \delta(v - v_n) \frac{P_n}{1 - P_0}. \quad (5)$$

The latter quantity can be determined experimentally as the histogram of velocities averaged over short time intervals. The average velocity of the cargo particle moving along the filament is then given by

$$v_{\text{eff}} = \sum_{n=1}^N v_n \frac{P_n}{1 - P_0}. \quad (6)$$

If the velocity of the cargo particle is independent of the number of bound motors,  $v_n = v$ , the effective velocity is equal to the single-motor velocity  $v$ .

**Effective unbinding rate.** Finally, the distribution of the number of bound motors implies also an explicit expression for the effective detachment or unbinding rate. In the stationary state, the effective binding and unbinding rates,  $\pi_{\text{eff}}$  and  $\epsilon_{\text{eff}}$ , fulfill the simple relation

$$\epsilon_{\text{eff}}(1 - P_0) = \pi_{\text{eff}} P_0 \quad (7)$$

where  $(1 - P_0)$  is again the probability that the cargo particle is bound to the filament through at least one motor. The effective binding rate is given by  $\pi_{\text{eff}} = \pi_0$  since the cargo-filament link is established as soon as one motor binds to the filament, so that  $\epsilon_{\text{eff}} = \pi_0 P_0 / (1 - P_0)$ .<sup>1</sup>

---

<sup>1</sup> This definition is equivalent to defining the effective unbinding rate as  $\epsilon_{\text{eff}} = \epsilon_1 P_1 / (1 - P_0)$ , i.e. as the unbinding rate of the last bound motor times the probability that a cargo particle bound to the filament is linked to this filament by a single motor.

With the distribution of the number of bound motors as given by Eq. (3), we obtain

$$\epsilon_{\text{eff}} = \epsilon_1 \left( 1 + \sum_{n=1}^{N-1} \prod_{i=1}^n \frac{\pi_i}{\epsilon_{i+1}} \right)^{-1}, \quad (8)$$

where the summation now starts with  $n = 1$ . For  $N = 2$  motors, this result reduces to  $\epsilon_{\text{eff}} = \epsilon_1 / (1 + \pi_1 / \epsilon_2)$ . An alternative derivation of (8) based on first passage times is presented in part A.1 of the Supporting Information.

**Distributions of binding times and walking distances.** The effective unbinding rate as given by Eq. (8) determines only the average time that the cargo particle is bound to the filament. The actual binding time  $\Delta t_b$  of the cargo particles is, however, a stochastic quantity which is governed by a certain probability distribution  $\tilde{\psi}_N(\Delta t_b)$ .

This probability distribution governs the passage from the state with one motor connecting the cargo to the filament at time  $t$  (immediately after binding) to the unbound state at time  $t + \Delta t_b$ . This distribution can be obtained by solving a recursion relation as shown in part A.2 of the Supporting Information. The general solution is a sum of exponentials,

$$\tilde{\psi}_N(\Delta t_b) = \sum_{i=1}^N e^{-z_i \Delta t_b} \text{Res}(-z_i), \quad (9)$$

where the scales  $-z_i$  of the exponentials and the prefactors  $\text{Res}(-z_i)$  are the poles and the corresponding residues, respectively, of a fraction of polynomials which is given in the Supporting Information. The time scales and prefactors are functions of the binding and unbinding rates and should not be considered as independent fit parameters when analyzing experimental data.

The distribution of the walking distances,  $\psi_N(\Delta x_b)$ , is obtained from the distribution of binding times by substituting  $\Delta t_b$  by  $\Delta x_b$ ,  $\epsilon_n$  by  $\epsilon_n / v_n$ , and  $\pi_n$  by  $\pi_n / v_n$ , i.e., by expressing the rates in units of (inverse) distance traveled rather than in units of inverse time. The distribution  $\psi_N(\Delta x_b)$  is therefore also given by a sum of  $N$  exponentials as in Eq. (9) and has the general form

$$\psi_N(\Delta x_b) = \sum_{i=1}^N e^{-z'_i \Delta x_b} \text{Res}(-z'_i). \quad (10)$$

The same substitution leads to an explicit expression for the average walking distance  $\langle \Delta x_b \rangle$  as given by

$$\langle \Delta x_b \rangle = \frac{v_1}{\epsilon_1} \left[ 1 + \sum_{n=1}^{N-1} \prod_{i=1}^n \frac{v_{i+1} \pi_i}{v_i \epsilon_{i+1}} \right] \quad (11)$$

which again applies to a cargo particle pulled by  $N$  motors.

### III. RESULTS

**Cargo particles with dilute motor coverage.** Let us now consider specific examples and specify the dependence of the rates  $\pi_n$  and  $\epsilon_n$  and of the velocity  $v_n$  on the number  $n$  of bound motors. First, we consider the case where the cargo particle is transported by  $N$  motor molecules which have well-separated anchor points on the particle surface and which, thus, do not experience mutual interactions. In the absence of an external load force, the parameters  $\epsilon_n$ ,  $\pi_n$  and  $v_n$  are then given by

$$\epsilon_n = n \epsilon, \quad \pi_n = (N - n) \pi_{\text{ad}}, \quad \text{and} \quad v_n = v, \quad (12)$$

where  $\epsilon$ ,  $\pi_{\text{ad}}$ , and  $v$  are the unbinding rate, the binding rate, and the velocity of a *single* motor, respectively.<sup>2</sup>

In the following, we use parameter values for kinesin motors as summarized in Table I to determine numerical results, but the general expressions can also be applied to other types of motors. Our model with rates as specified by Eq. (12) has three parameters which can be determined from the studies of single motor molecules: the velocity  $v$ , the unbinding rate  $\epsilon$ , and the binding rate  $\pi_{\text{ad}}$ . The first two quantities have been measured for many types of motors. For kinesin, the velocity is about  $1\mu\text{m/s}$  and the unbinding rate is about  $1/\text{s}$  [14, 15]. The binding rate is more difficult to measure. If  $\pi_{\text{ad}}$  is regarded as an unknown quantity, our results for the effective unbinding rate or the distribution of walking distances can be used to determine  $\pi_{\text{ad}}$  experimentally. Here, we use  $\pi_{\text{ad}} \simeq 5/\text{s}$  as measured for kinesins linking a membrane tube (which acts as the cargo particle) to a microtubule [11].

For the parameters as specified by (12), the general expression (4) for the average number of bound motors implies the explicit relation

$$N_{\text{b}} = \frac{(\pi_{\text{ad}}/\epsilon) [1 + (\pi_{\text{ad}}/\epsilon)]^{N-1}}{[1 + (\pi_{\text{ad}}/\epsilon)]^N - 1} N \quad (13)$$

which implies the simple asymptotic behavior  $N_{\text{b}} \approx \frac{(\pi_{\text{ad}}/\epsilon)}{1+(\pi_{\text{ad}}/\epsilon)} N$  for large  $N$ .

---

<sup>2</sup> In the present context, the binding rate  $\pi_{\text{ad}}$  corresponds to a motor which remains close to the filament because of the presence of the other motors connecting the cargo to the filament. In general, one should use  $\pi_n = (N - n)\pi_{\text{ad}}$  only for  $n \geq 1$  and specify  $\pi_0$  separately in order to account for the diffusion of the completely unbound cargo. The transport properties of the *bound* cargo particle are however independent of the choice for  $\pi_0$ .

Likewise, the general expression (11) for the average walking distance  $\langle \Delta x_b \rangle$  can be evaluated analytically which leads to

$$\langle \Delta x_b \rangle = \frac{v}{\epsilon_{\text{eff}}} = \frac{v}{N\pi_{\text{ad}}} \left[ \left( 1 + \frac{\pi_{\text{ad}}}{\epsilon} \right)^N - 1 \right]. \quad (14)$$

For strongly binding motors with  $\pi_{\text{ad}}/\epsilon \gg 1$ , the walking distance behaves as  $\langle \Delta x_b \rangle \approx \frac{v}{N\epsilon} (\pi_{\text{ad}}/\epsilon)^{N-1}$  and essentially increases exponentially with increasing number of motors. For weakly binding motors,  $\langle \Delta x_b \rangle \approx (v/\epsilon) [1 + \frac{N-1}{2} \frac{\pi_{\text{ad}}}{\epsilon}]$ , where the leading term  $v/\epsilon$  corresponds to the walking distance of a single motor.

Kinesin binds rather strongly with  $\pi_{\text{ad}}/\epsilon \simeq 5$ , so that the average walking distance, which is 1  $\mu\text{m}$  for a single motor, increases quickly with  $N$  and is 3.5  $\mu\text{m}$ , 14  $\mu\text{m}$ , 65  $\mu\text{m}$ , and 311  $\mu\text{m}$  for cargoes pulled by 2, 3, 4, or 5 motors, respectively. These large walking distances exceed the length of a single microtubule, but can still be realized if several microtubules are aligned in a parallel and isopolar fashion, so that, via unbinding and rebinding, the motors can step from one microtubule to another. Such an organization of microtubules is typical for axons [16] and has also been engineered in vitro [13].

Our results for the walking distance distributions of kinesin-pulled cargoes are shown in Fig. 2. With increasing motor number  $N$ , the slope of the distribution becomes increasingly steep for small walking distances, but the distribution becomes flatter and flatter for large walking distances. For more than 3 kinesins, the distribution is nearly constant for walking distances between 5 and 20  $\mu\text{m}$ , see Fig. 2.

If the motors are densely packed onto the cargo particle, exclusion effects [12, 17] modify the rates (12) as shown in part B and Fig. 6 of the Supporting Information. For typical motor numbers  $N \lesssim 10$ , the effect of exclusion on the velocity and the average walking distance is rather small. For very dense packing, however, a reduction of the velocity to about 35% of the value without exclusion is obtained, in agreement with experimental results [18].

**Movement against external load force.** Let us now consider cargo transport against a constant external force that could be applied, e.g., by optical tweezers or other single-molecule manipulation techniques. This force is shared equally between the  $n$  bound motors and induces an effective interaction of the motors, since, via the force-dependence, the transport parameters of the motors now depend on the presence of the other motors.



The velocity of a single motor decreases essentially linearly with the force imposed against the motor movement [19, 20, 21, 22]. We therefore use the linear force–velocity relation

$$v_n(F) = v \left( 1 - \frac{F}{nF_s} \right) \quad (15)$$

for  $0 \leq F \leq nF_s$  and take the velocity to be constant with  $v_n(F) = v$  for  $F < 0$  and  $v_n(F) = 0$  for  $F > F_s$ , compare [23]. The force scale  $F_s$  is given by the stall force at which a single motor stalls and stops moving. For kinesin, stall forces of  $F_s \simeq 5\text{--}7$  pN have been reported [19, 20, 21, 22]. In the following, we use the typical value  $F_s \simeq 6$  pN.

The force dependence of the unbinding rates  $\epsilon_n$  is given by

$$\epsilon_n(F) = n\epsilon \exp\left(\frac{F}{nF_d}\right). \quad (16)$$

as obtained from the measurements of the walking distance of a single motor as a function of load [24] in agreement with Kramers rate theory [25]. The detachment force  $F_d$ , which sets the force scale here, is, in general, not equal to the stall force, although both can be expected to have the same order of magnitude. The force scale  $F_d$  may be expressed as  $F_d \equiv k_B T/d$  which depends on the thermal energy  $k_B T$  and on the extension  $d$  of the potential barrier between the bound and unbound state. For kinesins, the length scale  $d$  has been reported to be  $d \simeq 1.3$  nm, so that the detachment force is  $F_d \simeq 3$  pN [24].

It is more difficult to estimate the force dependence of the binding rates  $\pi_n$  since there are no experimental data about this dependence. An external load force should lead to a decrease of the binding rate  $\pi_0$  from the unbound state but this binding rate does not affect the properties of the bound motor. The binding rates  $\pi_n$  with  $n \geq 1$ , on the other hand, are expected to depend only weakly on  $F$ . This is because a pulling motor, that is subject to a certain strain arising from  $F$ , will relax this strain as soon as it becomes unbound and will then rebind from such a relaxed state. In other words: unbinding and rebinding occur along different reaction coordinates, i.e., along different paths in configuration space. Therefore, we take the binding rates  $\pi_n$  with  $n \geq 1$  to be force-independent, so that  $\pi_n = (N - n)\pi_{\text{ad}}$  for  $n \geq 1$  as before. In Eqs. (15) and (16),  $v$  and  $\epsilon$  are the velocity and unbinding rate of a single motor in the absence of load, in agreement with Eq. (12). A similar type of binding/unbinding dynamics but

without the active movement in the bound state arises for the forced rupture of adhesion molecule clusters [26, 27, 28].<sup>3</sup>

The force–velocity relationships for cargo particles pulled by  $N$  motors are shown in Fig. 3(a). Even though the force–velocity curve is linear for a single motor, it is *non-linear* for  $N > 1$ , an effect that arises from the force-dependence of the unbinding rate which implies that the average number of bound motors decreases with increasing force, see Fig. 3(b). At high forces, a cargo particle is most likely bound to the filament by a single motor and this single motor then has a high unbinding rate, because it is pulled off from the filament by the total force.<sup>4</sup> For  $N > 2$ , the velocity decreases quickly for small and intermediate forces, but approaches zero rather slowly for forces close to the stall force. Indeed, the actual stall force for a cargo particle pulled by  $N$  motors is equal to  $N$  times the stall force  $F_s$  of a single motor, but the cargo movement will become undetectable already at much smaller forces.

The force-dependent increase of the unbinding rate is also reflected in the corresponding decrease of the average walking distance which is approximately exponential with increasing force  $F$  for  $N \geq 2$  as shown in Fig. 3(c).<sup>5</sup> For very strong forces which exceed a critical force  $F_c$ , the average walking distance becomes comparable to the motor step size  $\ell$  and the motors become unprocessive. This critical force can be estimated from the implicit equation  $\langle \Delta x_b(F_c) \rangle = \ell$ . For kinesin which has a step size  $\ell = 8\text{nm}$ , we obtain  $F_c = 5.7, 8.8, 10.6,$  and  $13.8$  pN for particles pulled by  $N = 1, 2, 3,$  and  $5$  motors, respectively. For  $N \geq 2$ , these values are considerably smaller than the corresponding stall forces. Force-dependent distributions of the walking distances are shown in Fig. 4.

In the presence of an external load force, the velocity depends on the number of motors which pull the cargo. This implies that the velocity of such a cargo particle is switched stochastically when a motor binds to or unbinds from the filament. The trajectory of such a cargo therefore consists of segments with constant velocity as has been observed recently for vesicles dragged through the cytoplasm [6, 7]. The distribution of these velocities is shown in Fig. 5.

---

<sup>3</sup> In the latter situation, the initial state is typically given by  $n = N$  rather than by  $n = 1$ .

<sup>4</sup> For high forces with  $F \gtrsim 25\text{pN}$ , the effective unbinding rate, is given by  $\epsilon_{\text{eff}} \approx \epsilon_1(F) = \epsilon e^{F/F_d}$ , independent of the number of motors.

<sup>5</sup> For  $N = 1$ , the walking distance is given by  $\langle \Delta x_b(F) \rangle = (v/\epsilon)(1 - F/F_s) e^{-F/F_d}$ .

With increasing load force, the observed velocities decrease, but in addition, the velocity distribution  $P(v)$  becomes broader and develops several peaks. The latter feature is again consistent with the in vivo experiments in Refs. [6, 7].

#### IV. DISCUSSION AND APPLICATIONS

We have presented a theoretical study of the transport properties of cargo particles which are pulled by several molecular motors in a cooperative fashion. Let us now discuss some applications of our results to cellular systems.

The most prominent example for long-range transport over distances which by far exceed the walking distances of single motors is the transport in axons [16]. The cargo particles which belong to the *slow* transport component such as neurofilaments exhibit alternating periods of directed movement with velocities of the order of  $1\mu\text{m/s}$  and pausing periods where essentially no movement can be detected, so that their effective velocity is of the order of  $\sim 10^{-3} - 10^{-2}\mu\text{m/s}$  or  $\sim 0.1 - 1$  mm per day. The walking distances of the active movements are typically a few microns, see [29, 30]. These observations are consistent with the assumption that these slow cargoes are transported by one or two motors. On the other hand, cargo particles of *fast* axonal transport such as vesicles move with velocities of  $\sim 1\mu\text{m/s}$  over distances of at least centimeters. Using Eq. (14), we can estimate that the cooperation of 7–8 kinesin motors is sufficient for a walking distance in the centimeter range. A walking distance of  $\sim 1\text{m}$  as necessary in the longest axons is obtained if 10 motors drive the movement.

Our theory also gives a quantitative explanation for the effect of microtubule-associated proteins (MAPs) such as the tau protein on the processivity of cargo particles. On the one hand, the presence of tau reduces the binding rate of kinesin to microtubules in single-molecule experiments, but has no effect on the velocity and walking distance of the bound kinesins [31]. On the other hand, the movements of vesicles in cells transfected with tau exhibit reduced walking distances [32]. It has been proposed [31] that these apparently contradictory experimental findings can be reconciled if the vesicles with reduced walking distance were transported by several motors. Our theory supports this idea, since Eq. (11) implies that the walking distance of a cargo particle pulled by more than one motor is affected by changes in the binding rate. At a ratio of two tau molecules per tubulin dimer, the binding rate of a single kinesin

molecule is reduced to about 50 percent of its value in the absence of tau [31]. For cargoes pulled by 2, 3, and 4 kinesin motors, this reduction of the binding rate implies a reduction of the walking distance to 64, 40, and 16 percent of the corresponding value in the absence of tau, respectively.

Finally, we have calculated the transport properties of cargo particles pulled by several motors against an external load force. This situation is accessible to in vitro experiments, using, for example, bead assays and optical traps which exert constant forces. For such experiments, our theory makes quantitative predictions about the force-velocity relationships, the walking distances, and the distribution of the instantaneous cargo velocities.

In addition, our theory can be applied to the movement of large organelles in cells which experience viscous forces of a few piconewtons comparable to the stall force of a single motor [9]. If the cargo particle moves with velocity  $v_n$ , it experiences the Stokes force  $F_n = \gamma v_n$  where  $\gamma$  is the corresponding friction coefficient. In the presence of such a force, our relation (15) leads to

$$v_n = \frac{v}{1 + \gamma v / (nF_s)} \approx n \frac{F_s}{\gamma}, \quad (17)$$

where the asymptotic equality applies to large friction coefficients  $\gamma$ . For such a situation, two groups [6, 7] have recently measured the distribution of the instantaneous velocities as given by Eq. (5). They found that the vesicles switch between different values of the velocity which are peaked at integer multiples of the smallest observed velocity. If the friction coefficient is large compared to  $nF_s/v$  such a linear behavior is indeed predicted by Eq. (17).

In summary, we have presented a theoretical study of the cooperative transport of cargo particles that are pulled by up to  $N$  molecular motors. We have determined the transport properties of these cargo particles such as their effective velocity and average walking distance (or run length). The latter quantity is strongly affected by the maximal number  $N$  of pulling motors, and the cooperation of several motors enables efficient transport over large distances. Our approach provides a quantitative theoretical basis for the interpretation of a number of recent experiments and makes quantitative predictions which can be tested experimentally. The theoretical framework introduced here can be extended to more complex situations such as the transport of cargo particles that are attached to several species of motors. These different species may have different velocities or may even move in opposite directions. Likewise, our theory can be extended to load forces that depend on the displacement of the cargo

particle or change with time. A relatively simple example for such a variable load force is provided by laser traps, which are used in motility assays in order to exert harmonic force potentials for small particle displacements. More complex examples are found for the cytoskeletal transport in biological cells, where the cargo particle is pulled through a meshwork of membranes and filaments that can act as steric barriers or adhesive surfaces and, thus, can exert various types of position-dependent forces on this particle.

### Acknowledgments

The authors thank Janina Beeg, Melanie Müller, Thorsten Erdmann, and Ulrich Schwarz for stimulating discussions.

- 
- [1] Howard, J. (2001) *Mechanics of Motor Proteins and the Cytoskeleton* (Sinauer Associates, Sunderland, MA).
  - [2] Schliwa, M., editor (2003) *Molecular motors* (Wiley-VCH, Weinheim).
  - [3] Miller, R. H. & Lasek, R. J. (1985) *J. Cell Biol.* **101**, 2181–2193.
  - [4] Ashkin, A., Schütze, K., Dziedzic, J. M., Euteneuer, U., & Schliwa, M. (1990) *Nature* **348**, 346–348.
  - [5] Gross, S. P., Welte, M. A., Block, S. M., & Wieschaus, E. F. (2002) *J. Cell Biol.* **156**, 715–724.
  - [6] Hill, D. B., Plaza, M. J., Bonin, K., & Holzwarth, G. (2004) *Eur. Biophys. J* **33**, 623–632.
  - [7] Kural, C., Kim, H., Syed, S., Goshima, G., Gelfand, V. I., & Selvin, P. R. (2005) *Science* **305**, 1469–1472.
  - [8] Kuznetsov, S. A., Langford, G. M., & Weiss, D. G. (1992) *Nature* **356**, 722–725.
  - [9] Luby-Phelps, K. (2000) *Int. Rev. Cytol. – Survey Cell Biol.* **192**, 189–221.
  - [10] Koster, G., VanDuijn, M., Hofs, B., & Dogterom, M. (2003) *Proc. Natl. Acad. Sci. USA* **100**, 15583–15588.
  - [11] Leduc, C., Campàs, O., Zeldovich, K. B., Roux, A., Jolimaitre, P., Bourel-Bonnet, L., Goud, B., Joanny, J.-F., Bassereau, P., & Prost, J. (2004) *Proc. Natl. Acad. Sci. USA* **101**, 17096–17101.
  - [12] Lipowsky, R., Klumpp, S., & Nieuwenhuizen, T. M. (2001) *Phys. Rev. Lett.* **87**,

- 108101.
- [13] Böhm, K. J., Stracke, R., Mühlig, P., & Unger, E. (2001) *Nanotechnology* **12**, 238–244.
  - [14] Block, S. M., Goldstein, L. S. B., & Schnapp, B. J. (1990) *Nature* **348**, 348–352.
  - [15] Vale, R. D., Funatsu, T., Pierce, D. W., Romberg, L., Harada, Y., & Yanagida, T. (1996) *Nature* **380**, 451–453.
  - [16] Goldstein, L. S. B. & Yang, Z. (2000) *Annu. Rev. Neurosci.* **23**, 39–71.
  - [17] Klumpp, S., Nieuwenhuizen, T. M., & Lipowsky, R. (2005) *Biophys. J.* **88**, 3118–3132.
  - [18] Böhm, K. J., Stracke, R., & Unger, E. (2000) *Cell Biol. Int.* **24**, 335–341.
  - [19] Svoboda, K. & Block, S. M. (1994) *Cell* **77**, 773–784.
  - [20] Hunt, A. J., Gittes, F., & Howard, J. (1994) *Biophys. J.* **67**, 766–781.
  - [21] Kojima, H., Muto, E., Higuchi, H., & Yanagida, T. (1997) *Biophys. J.* **73**, 2012–2022.
  - [22] Visscher, K., Schnitzer, M. J., & Block, S. M. (1999) *Nature* **400**, 184–189.
  - [23] Block, S. M., Asbury, C. L., Shaewitz, J. W., & Lang, M. J. (2003) *Proc. Natl. Acad. Sci. USA* **100**, 2351–2356.
  - [24] Schnitzer, M. J., Visscher, K., & Block, S. M. (2000) *Nature Cell Biol.* **2**, 718–723.
  - [25] Kramers, H. A. (1940) *Physica* **7**, 284–304.
  - [26] Bell, G. I. (1978) *Science* **200**, 618–627.
  - [27] Seifert, U. (2000) *Phys. Rev. Lett.* **82**, 2750–2753.
  - [28] Erdmann, T. & Schwarz, U. S. (2004) *Phys. Rev. Lett.* **92**, 108102.
  - [29] Wang, L., Ho, C.-L., Sun, D., Liem, R. K. H., & Brown, A. (2000) *Nature Cell Biol.* **2**, 137–141.
  - [30] Shah, J. V. & Cleveland, D. W. (2002) *Curr. Opin. Cell Biol.* **14**, 58–62.
  - [31] Seitz, A., Kojima, H., Oiwa, K., Mandelkow, E.-M., Song, Y.-H., & Mandelkow, E. (2002) *EMBO J.* **21**, 4896–4905.
  - [32] Trinczek, B., Ebner, A., Mandelkow, E.-M., & Mandelkow, E. (1999) *J. Cell Sci.* **112**, 2355–2367.

Parameter	Symbol	Value for kinesin	Reference
Velocity	$v$	1 $\mu\text{m/s}$	[14, 15]
Unbinding rate	$\epsilon$	1/s	[14, 15]
Binding rate	$\pi_{\text{ad}}$	5/s	[11]
Stall force	$F_s$	6pN	[22, 24]
Detachment force	$F_d$	3pN	[24]

TABLE I: Model parameters for single motors and values for conventional kinesin.

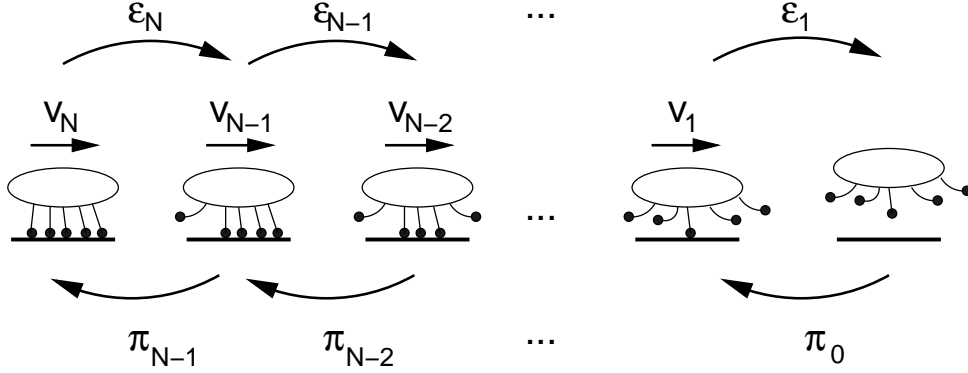


FIG. 1: A cargo particle is transported cooperatively by  $N$  molecular motors along a filament. The motors are firmly attached to the cargo but unbind from and rebind to the filament. Each state of the system, denoted by  $|n\rangle$ , is characterized by the number  $n$  of bound motors that pull on the cargo particle. The latter number can vary between  $n = N$  (on the left) and  $n = 0$  (on the right). In state  $|n\rangle$ , the cargo particle has velocity  $v_n$ , a motor unbinds from the filament with rate  $\epsilon_n$ , and an additional motor binds to the filament with rate  $\pi_n$ .

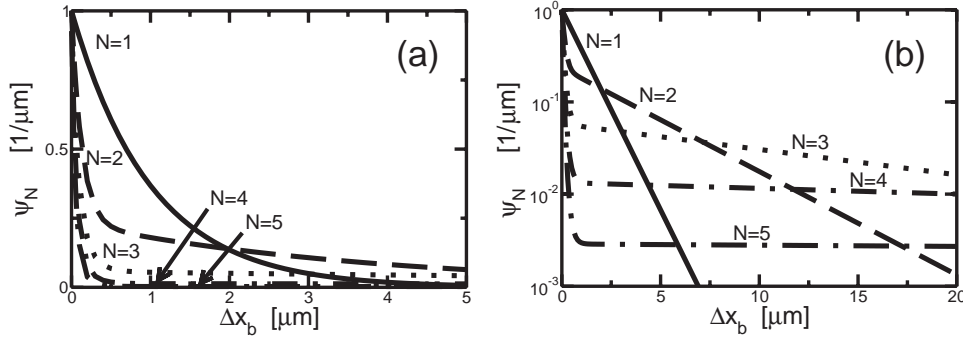


FIG. 2: Probability distribution  $\psi_N$  of walking distance  $\Delta x_b$  for cargo particles pulled by  $N = 1, 2, 3, 4, 5$  kinesin motors with parameters as given in Table I. The same distributions are plotted on a linear scale in (a) and on a semi-logarithmic scale in (b).



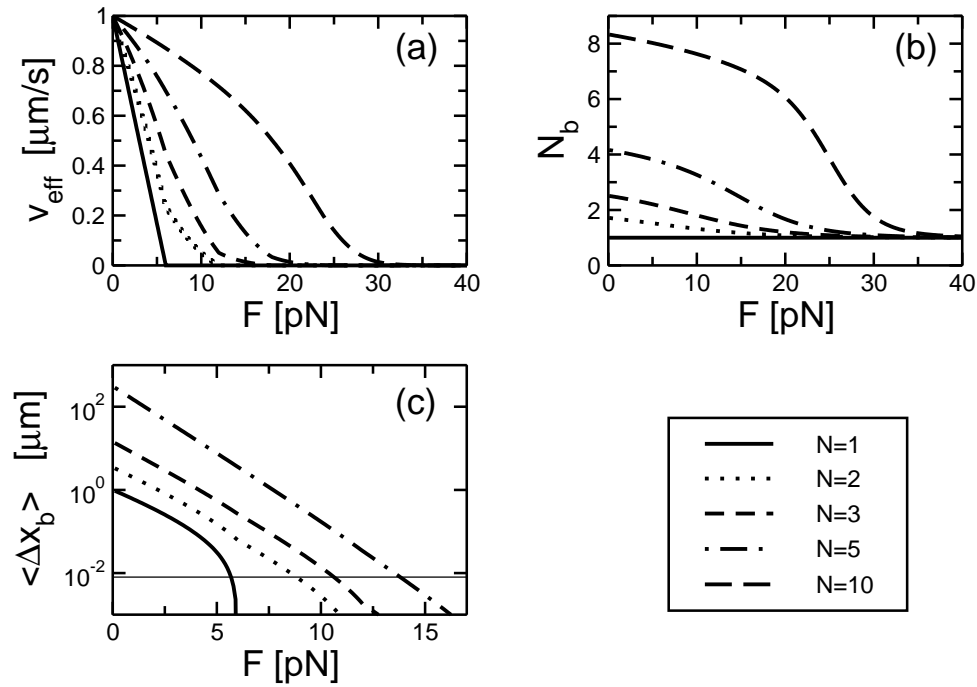


FIG. 3: Transport properties of cargo particles pulled by up to  $N$  motors against a constant external load force  $F$ : (a) Average velocity  $v_{\text{eff}}$ ; (b) Average number  $N_b$  of bound motors; and (c) Average walking distance  $\langle \Delta x_b \rangle$ . The chosen parameter values are for kinesin as in Table I. The horizontal line in (c) indicates the step size of 8nm. For forces for which  $\langle \Delta x_b \rangle$  becomes comparable to or smaller than the step size, the motors become unprocessive.

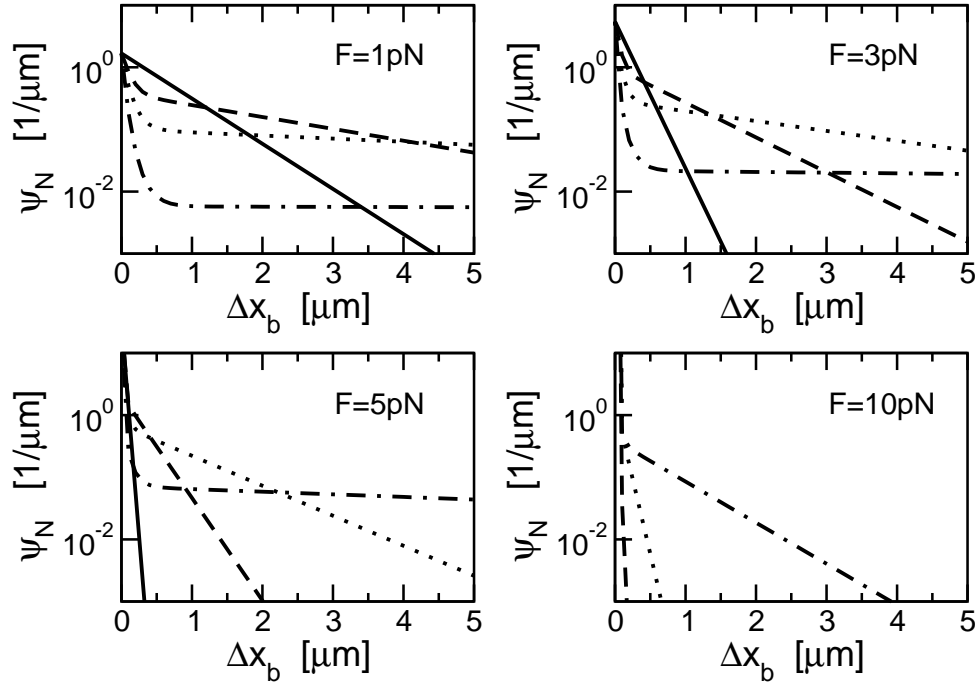


FIG. 4: Probability distribution  $\psi_N$  of walking distance  $\Delta x_b$  for cargo particles pulled by up to  $N = 1$  (solid lines), 2 (dashed lines), 3 (dotted lines), and 5 (dash-dotted lines) motors against an external load force  $F$ . For  $F = 10$  pN, cargoes pulled by a single motor do not move, and the distribution  $\psi_N$  contains a delta function at  $\Delta x_b = 0$ . The distributions are plotted on a semi-logarithmic scale as in Fig. 2(b).

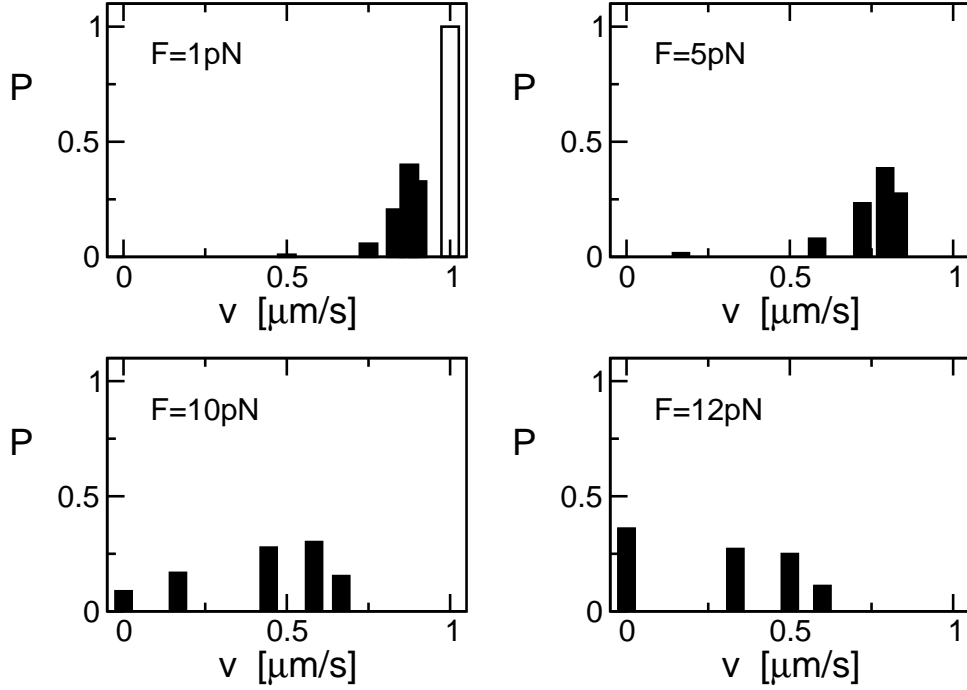


FIG. 5: Probability distribution  $P$  of the instantaneous velocity  $v$  for cargo particles that are pulled by  $N = 5$  motors in the presence of an external load force  $F$ . The chosen parameter values are given in Table I and apply to kinesin. The white bar in the graph for  $F = 1$  pN indicates the distribution for vanishing external force. For  $F = 10$  pN and  $F = 12$  pN, the particles are stalled with a non-zero probability  $P(v = 0)$ , because no movement occurs if the cargo particle is pulled by a single motor for  $F = 10$  pN or by one or two motors for  $F = 12$  pN.

# Supporting text

## A. TECHNICAL ASPECTS OF THE CALCULATIONS

### A.1. Mean First Passage Times

The effective unbinding rate as given by Eq. 8 has been derived by a simple equilibrium argument. The same equation can also be obtained by calculating the mean first passage time. Let us denote by  $T_{m,N}$  the mean first passage time to the state  $|0\rangle$  with no bound motor if we start from state  $|m\rangle$  with  $m$  bound motors at time  $t = 0$  (the second index  $N$  indicates the total number of motors). The effective unbinding rate is then given by  $1/T_{1,N}$ , since the cargo particle first binds to the filament through a single motor.

The first passage times fulfill the recursion relations

$$T_{m,N} = \frac{1}{\epsilon_m + \pi_m} + \frac{\pi_m}{\epsilon_m + \pi_m} T_{m+1,N} + \frac{\epsilon_m}{\epsilon_m + \pi_m} T_{m-1,N} \quad (\text{S.18})$$

for  $m \neq 0, N$ , see, e.g., ref. 1, with the boundary recursions

$$T_{N,N} = \frac{1}{\epsilon_N} + T_{N-1,N} \quad \text{and} \quad (\text{S.19})$$

$$T_{0,N} = 0. \quad (\text{S.20})$$

Because of the boundary condition  $T_{0,N} = 0$ , the recursion relation Eq. S.1 with  $m = 1$  can be used to express  $T_{2,N}$  in terms of  $T_{1,N}$ . Next, starting from Eq. S.1 with  $m = 2$  and using the relation between  $T_{2,N}$  and  $T_{1,N}$ , we can also express  $T_{3,N}$  in terms of  $T_{1,N}$ . Iteration of this procedure leads to explicit expressions for  $T_{m,N}$  in terms of  $T_{1,N}$ . Finally, when these expressions are used in Eq. S.2, we obtain an implicit equation for  $T_{1,N}$ , which is solved by

$$T_{1,N} = \frac{1}{\epsilon_1} \left( 1 + \sum_{i=1}^{N-1} \prod_{n=1}^i \frac{\pi_n}{\epsilon_{n+1}} \right), \quad (\text{S.21})$$

which is exactly the inverse of Eq. 8.

### A.2. Distribution of Unbinding Times

To calculate the distribution of unbinding times, we consider the probability distribution for the passage from state  $|m\rangle$  with  $m$  bound motors at time  $t = 0$  to the unbound state  $|0\rangle$  at time  $t$ , which we denote by  $\tilde{\psi}_{m,N}(t)$ . The distribution

of unbinding times is then given by  $\tilde{\psi}_N(\Delta t_b) \equiv \tilde{\psi}_{1,N}(t = \Delta t_b)$  since the initial bound state of the cargo particle is provided by state  $|1\rangle$  with  $m = 1$  for which the particle is bound to the filament by a single motor.

The probability distributions  $\tilde{\psi}_{m,N}(t)$  fulfill the recursion relations

$$\tilde{\psi}_{m,N}(t) = \int_0^t e^{-(\epsilon_m + \pi_m)\tau} \left[ \pi_m \tilde{\psi}_{m+1,N}(t - \tau) + \epsilon_m \tilde{\psi}_{m-1,N}(t - \tau) \right] d\tau \quad (\text{S.22})$$

for  $m \neq 0, N$ ,

$$\tilde{\psi}_{N,N}(t) = \int_0^t e^{-\epsilon_N \tau} \epsilon_N \tilde{\psi}_{N-1,N}(t - \tau) d\tau, \quad \text{and} \quad (\text{S.23})$$

$$\tilde{\psi}_{0,N}(t) = \delta(t). \quad (\text{S.24})$$

These recursion relations are obtained by considering the first binding/unbinding event explicitly, summing over the two possibilities for this step (to  $m \pm 1$ ), and integrating over all possible times  $\tau$  at which this first event occurs. The exponential terms express the probability that no binding/unbinding event occurred until the time  $\tau$ .

Using Laplace transforms, we can transform the convolution integrals into algebraic equations and iteratively obtain all the Laplace transformed distributions  $\tilde{\psi}_{m,N}(s)$ . The solution is given by a finite continued fraction of depth  $N$ , which has the form

$$\tilde{\psi}_{1,N}(s) = \frac{\epsilon_1}{\epsilon_1 + s + \pi_1 \left( 1 - \frac{\epsilon_2}{\epsilon_2 + s + \pi_2 \left( 1 - \frac{\epsilon_3}{\dots + \pi_{N-1} \left( 1 - \frac{\epsilon_N}{\epsilon_N + s} \right) \dots \right)} \right)}, \quad (\text{S.25})$$

see chapter 9 of ref. 2.

In general, the inverse Laplace transform of Eq. **S.8** can be expressed as

$$\tilde{\psi}_{1,N}(t) = \sum_{i=1}^N e^{-z_i t} \text{Res}(-z_i), \quad (\text{S.26})$$

where the parameters  $-z_i$  are the poles of  $\tilde{\psi}_{1,N}(s)$  and  $\text{Res}(-z_i)$  are the corresponding residues (see ref. 3). All poles  $-z_i$  are real and negative. Using the definition  $\tilde{\psi}_N(\Delta t_b) \equiv \tilde{\psi}_{1,N}(t = \Delta t_b)$  in the relation Eq. **S.9**, we obtain the binding time distribution as given by Eq. **9**.

In general, the poles and the residues have to be calculated numerically, but in the two simplest cases,  $N = 1$  and  $N = 2$ , the inverse Laplace transform can be obtained in closed form. For  $N = 1$ , we can check that we recover the single

exponential  $\tilde{\psi}_{1,1}(t) = \epsilon_1 e^{-\epsilon_1 t}$ , and for  $N = 2$  the first passage time distribution is given by

$$\begin{aligned} \tilde{\psi}_{1,2}(t) = & \frac{\epsilon}{2} \left[ \left( 1 - \frac{\epsilon_1 + \pi_1 - \epsilon_2}{R} \right) e^{-\frac{1}{2}(\epsilon_1 + \epsilon_2 + \pi_1 - R)t} \right. \\ & \left. + \left( 1 + \frac{\epsilon_1 + \pi_1 - \epsilon_2}{R} \right) e^{-\frac{1}{2}(\epsilon_1 + \epsilon_2 + \pi_1 + R)t} \right] \end{aligned} \quad (\text{S.27})$$

with  $R \equiv \sqrt{(\epsilon_1 + \epsilon_2 + \pi_1)^2 - 4\epsilon_1\epsilon_2}$ .

## B MUTUAL EXCLUSION OF MOTORS

In general, several motor molecules, which are bound to a certain cargo particle, may compete for the same binding site of the filament. Such a competition may arise, for example, because the motor molecules are densely packed on the cargo particle or because they move along a single protofilament of the microtubule. In such a situation, mutual exclusion or hard core repulsion between the motors should to be taken into account. Exclusion reduces the binding of motors to the filament and the velocity of the bound motors (4,5). Within a mean-field approximation, these two effects can be incorporated into our model by using modified binding rates  $\pi_n$  and modified bound state velocities  $v_n$  as given by

$$\pi_n = (N - n)\pi_{\text{ad}} \left[ 1 - \frac{n}{N_s} \right] \quad \text{and} \quad v_n = v \left[ 1 - \frac{n-1}{N_s-1} \right] \quad (\text{S.28})$$

for  $n \leq N_s$  where  $N_s$  is the number of accessible binding sites that the motors can reach for a given position of the cargo particle. The terms  $[1 - n/N_s]$  and  $[1 - (n-1)/(N_s-1)]$  describe the probability that the site to which a motor attempts to bind or to move is not occupied by another motor.<sup>6</sup> For  $n \geq N_s$ , all binding sites that could be reached by the motors are occupied, so that  $\pi_n = 0$  for  $n \geq N_s$ . The unbinding rates  $\epsilon_n$  are unaffected by exclusion and are again given by  $\epsilon_n = n\epsilon$ . If the number of accessible binding sites  $N_s$  is much larger than the number of motors attached to the cargo particle, the motors are effectively noninteracting, and Eq. (S.28) can be approximated by Eq. **12**.

---

<sup>6</sup> The difference between these two expressions arises from a finite-size effect. When an unbound motor attempts to bind to the state  $|n\rangle$ , it encounters  $n$  out of  $N_s$  binding sites that are already occupied. In contrast, a bound motor in state  $|n\rangle$  ‘feels’ only  $n-1$  motors, which are bound to  $n-1$  out of the remaining  $N_s-1$  binding sites.

For typical cargoes such as beads or vesicles with diameters between 100 nm and 1  $\mu\text{m}$ , we can estimate the number of binding sites within the contact zone of the cargo particle to be of the order of 50–150, while the number of motors is typically 1–10. For these motor numbers and for the parameter values corresponding to kinesin, exclusion effects are rather small. Inspection of Fig. 6a shows that the average velocity is reduced by a few percent as compared to noninteracting motors. The average walking distance is more sensitive to exclusion, but still of the same order of magnitude as for noninteracting motors. For example, for  $N = 5$ , the walking distance which is  $\simeq 310$  nm without exclusion is reduced to 280 nm, see Fig. 6b.

If motors are closely packed on the cargo particle, i.e. for  $N \simeq N_s$ , a reduction of the velocity to about 35 percent of the value without exclusion is obtained as shown in Fig. 6a. For very high motor densities, a reduction of the velocity of the order of 50 percent has indeed been observed both in microtubule gliding assays (6) and bead assays (J. Beeg, private communication) for kinesin.

In principle, exclusion implies that the walking distance exhibits a maximum as a function of the number of motors, since at very large motor numbers, the velocity approaches zero. Using the rates given by Eq. S.11 in Eq. 11, we find, however, that this maximum occurs at walking distances that are far too large to be experimentally accessible.

1. van Kampen, N. G. (1992) *Stochastic Processes in Physics and Chemistry* (Elsevier, Amsterdam).
2. Risken, H. (1989) *The Fokker–Planck Equation* (Springer, Berlin) 2nd Ed.
3. Schiff, J. L. (1999) *The Laplace Transform: Theory and Applications* (Springer, New York).
4. Lipowsky, R., Klumpp, S. & Nieuwenhuizen, T. M. (2001) *Phys. Rev. Lett.* **87**, 108101.
5. Klumpp, S., Nieuwenhuizen, T. M. & Lipowsky, R. (2005) *Biophys. J.* **88**, 3118–3132.

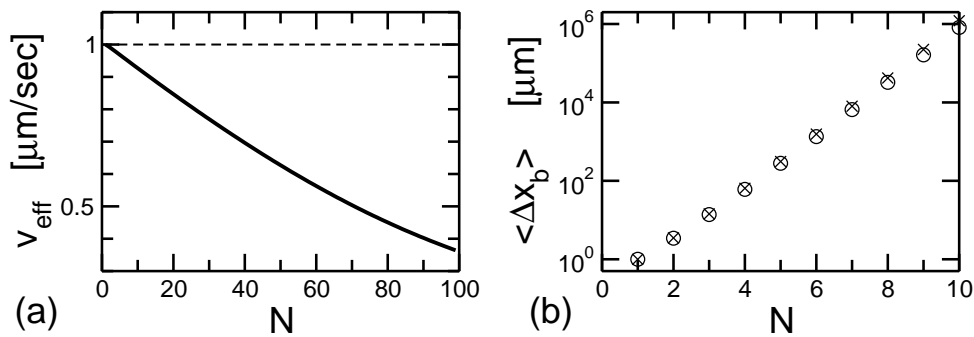


FIG. 6: Exclusion effects: (a) Average velocity  $v_{\text{eff}}$  and (b) average walking distance  $\langle \Delta x_b \rangle$  as functions of the number  $N$  of motors attached to the cargo. The chosen parameter values are those of kinesin as described in the text. The number of binding sites which are accessible to the motors for a given position of the cargo particle is  $N_s = 100$  as appropriate for a cargo with radius  $\sim 1\mu\text{m}$  [solid line in (a) and circles in (b)]. The values indicated by the dashed line in (a) and the crosses in (b) are obtained if exclusion effects are not taken into account. For typical motor numbers  $N \lesssim 10$ , direct comparison shows that exclusion effects are small.